

Finding the Optimal Detector Location at Metering Roundabouts using AIMSUN

Hong Ki AN^{a*}, Wen Long YUE^b and Branko STAZIC^c, Chengjiang LI^d

^{a, b, d} *School of Natural and Built Environments, University of South Australia, South Australia, 5095, Australia*

^a *Email: hong_ki.an@mymail.unisa.edu.au*

^b *Email: Wen.Yue@unisa.edu.au*

^c *School of Computer Science, Engineering and Mathematics, Flinders University, South Australia, 5001, Australia; Email: branko.stazic@flinders.edu.au*

^d *Email: chengjiang.li@mymail.unisa.edu.au*

Abstract: At metering roundabouts, the determination of detector location is a crucial task because signal phase time can be adjusted according to its position. Akçelik (2005, 2011) has suggested a range of 50–120 meters for detector location; however, no specific guideline for deciding optimal detector location is provided. This paper, therefore, presents a way of finding the optimal detector location at metering roundabouts based on TS351 (Old Belair Road/Blythewood Road, Adelaide, South Australia) using AIMSUN7 software. Modelling and calibration methods are also reported. For more accurate evaluation, three resources (drone survey data, SCATS data and DPTI documents) were used on 17th November, 2015. The results from the analysis show that detector location at 200 meters can generate minimum queuing length for the entire roundabout during the morning peak periods and detector location at 50 meters leads to longer queuing length.

Keywords: Metering roundabouts, Detector location, Queuing length, AIMSUN, SCATS, Drone survey.

1. INTRODUCTION

Roundabouts can enhance intersection performance under balanced traffic conditions; thus, signalized intersections are being replaced by roundabouts in order to reduce congestion. However, unbalanced traffic conditions may generate delays on one or two approaches as many real world cases show (Akçelik 2004; Hummer et al. 2014; Stevens 2005). This is because entering vehicles from a dominant approach may be stopped by circulating vehicles, and as a result have fewer chances of finding a safe gap between the circulating vehicles. This phenomenon leads to longer queues and delays for other approaches, and consequently the entire intersection carries lower traffic volumes.

In order to convert traffic conditions from unbalanced to balanced, signalized roundabouts where traffic signals are installed can be considered, with the metering roundabout in particular having a good benefit-cost ratio (Akçelik 2006a).

As illustrated in Figure 1, the operational concept of a simple signal metering roundabout is that when the queue reaches the queue detector on the controlling approach for a pre-determined duration, the traffic signal on the metered approach changes to red. Consequently, vehicles from the controlling approach are given opportunities to enter the roundabout. Furthermore, when the roundabout starts to operate in metering mode, a stop-line

* Corresponding author

setback in the range of 15–25 meters needs to be implemented on the metered approach for safety. With respect to a metering roundabout, the determination of the detector location is very important, because queuing lengths on each approach can be affected by when the signal should be actuated and the signal's green/red time, which is determined by when the queue hits the detector on the controlling approach.

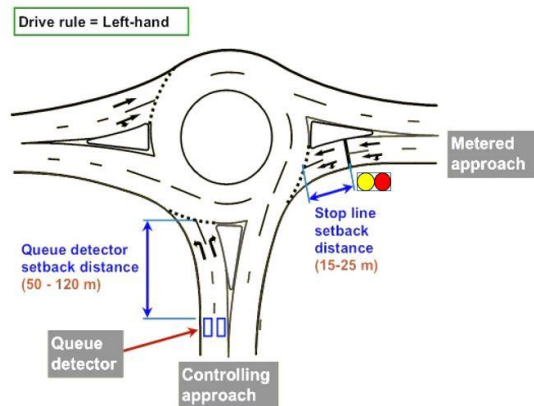


Figure 1. Operation concept of a metering roundabout

Reproduced from Akçelik 2006b)

Over the past decades, there have been several studies regarding the outstanding performance of metering roundabouts. However, these studies have concentrated on the evaluation of controlling and metered approaches only. In addition, there have been minimal studies about the determination of detector location, which is a key factor in a metering roundabout. Queuing length on each approach can be affected by the relationship between detector location and signal phase time. In order to determine detector location, Akçelik (2005, 2011) suggested a range of 50 to 120 meters from the stop line for metering roundabouts, which is too big a range to provide clear guidelines. Moreover, finding the optimal detector location using AIMSUN has not previously been conducted.

Therefore, this study modelled a metering roundabout based on Old Belair Road/Blythewood Road metering roundabout (known as TS351) to find the optimal detector location using AIMSUN7 software. For accurate analysis, two drones for queuing length recording, SCATS data for traffic volumes, signal phase time, and South Australian Department of Planning, Transport and Infrastructure (DPTI) documents were used on 17th November, 2015.

2. LITERATURE REVIEW

Studies regarding roundabouts, particularly on capacity evaluation, have been focused on operational effectiveness between normal roundabouts and metering roundabouts. In order to compare roundabout performance, evaluation with software (e.g. microscopic simulation: VISSIM, AIMSUN and Paramics, and analytical model: SIDRA) has been widely used (Zadid & Yue 2009).

Akçelik (2006b) performed a case study to compare delays and queues between normal and metering roundabouts using SIDRA software. The 3-leg intersection of Nepean Highway and McDonald Street, Victoria, Australia, was selected as a research case as this intersection faced a congestion problem caused by unbalanced traffic flows in the morning peak. Akçelik

compared five scenarios (no metering, only display red signal, only display blank signal, combination of red and blank, and signalized intersection) for the effectiveness of a metering roundabout. He concluded that a metering roundabout is the most effective control device in relation to cost and performance, and that it can reduce CO₂ emissions and fuel consumption.

Geers et al. (2009) conducted a study on metering roundabouts with the aim of analyzing delay times. It was based on the Yallah roundabout, Sydney, Australia, which experienced unbalanced traffic conditions during morning and afternoon peak times. In order to obtain field data, the state of the traffic, such as queue length, on each approach was observed using video cameras. The delay time at the roundabout was derived using the microscopic simulation model Paramics. The results showed that the use of metering can decrease delay time significantly compared with non-metering.

Ahn (2012) studied metering roundabouts to investigate operational effectiveness and traffic signal positions in accordance with changing entry traffic volumes. The study used SIDRA software based on a 4-leg roundabout with one circulatory lane (diameter: 25m, circulatory lane width: 5m, entering speed: 20km/h). Key parameters (critical gap and follow-up headway) were assumed to be in the range of 4.1–4.6 seconds and 2.6–3.1 seconds respectively. The author entered 800–2,200 pcph of entry volume on the controlling approach. The research found that when the traffic volume of the controlling approach was less than 50% of total entry volume, signal metering was ineffective. In addition, when the entry volume was more than 2,000 pcph, the average delay and queue length were increased. If the entry volume was more than 70%, the average delay and queuing length decreased. Furthermore, when the metered approach was located on the right side of the controlling approach, it led to more efficient results. This means that metered approaches need to be positioned adjacent and upstream of controlling approaches.

3. STUDY SITE

As mentioned earlier, to find the optimal detector location using AIMSUN software a real metering roundabout was duplicated. TS351 is a roundabout at Old Belair Road and Blythewood Road, located in the southern part of the Adelaide metropolitan area, South Australia, and the location is shown in Figure 2.



Figure 2. Location of TS351

TS351 is a 4-leg multi-lane roundabout. A feature of this roundabout is that in the morning peak it services many commuters, especially on the southern approach where the vehicle storage area is shorter than on the other approaches. In addition, the southern approach joins another local road close to the roundabout. Therefore, the detectors are installed 115 meters from the stop line on the southern (controlling approach) and two traffic signals on the northern and eastern (metered approach) are activated to reduce queuing length on the southern approach (the majority of drivers tended to violate the red signal and traffic volume is low on the eastern approach, thus this paper considers only one signal on the northern approach).

This roundabout serves commuters from the southern part of Adelaide along a major transport corridor. Due to extremely unbalanced traffic flows, it uses a typical metering roundabout: the metering system only operates in the peak periods, and it follows normal roundabout rules during non-peak periods.

3.1 Queuing length by drone survey

The purpose of using drones was to trace the back of queue on each approach, which was observed using two drones. The measured distance was applied for model calibration. The survey was conducted between 07:50 and 08:50. Figure 3 shows the footage from the two drones and the time stamp that identifies the video recording start time.



Figure 3. Drone footage

For the one-hour duration of the survey, queuing length from the northern approach was longer than the other approaches, as described in Table 1. On the other hand, queuing length on the eastern approach was less than 20 meters during the survey period.

Table 1. Queuing length

Time	**Northern (m)	*Southern (m)	Western (m)	**Eastern (m)
07:50–07:55	680	67	58	20
07:55–08:00	768	67	40	10
08:00–08:05	700	53	58	10
08:05–08:10	906	67	58	10
08:10–08:15	790	58	40	10
08:15–08:20	1003	153	115	0
08:20–08:25	835	170	170	7
08:25–08:30	507	128	120	7
08:30–08:35	650	135	180	10
08:35–08:40	60	160	225	7
08:40–08:45	45	130	230	0
08:45–08:50	95	45	85	7

Note: *Controlling approach, **Metered approach

In respect to the southern (controlling) approach, Table 1 shows that the queuing length was longer than 128 meters between 08:15 and 08:45. This means that it was only in those periods that the roundabout was operated with a metering signal, with the fixed time signal running for the remaining periods (07:50–08:15 and 08:45–08:50).

3.2 SCATS VS and SM data

Table 2 presents traffic volumes on each approach during the survey periods between 07:50 and 08:50. The hourly volume was recorded as 2,258 vehicles (i.e. northern 740 veh/h, southern 904 veh/h, western 577 veh/h and eastern 37 veh/h).

Table 2. Arrival volume

Time	Northern (veh)	Southern (veh)	Western (veh)	Eastern (veh)	Total (veh)
07:50–07:55	64	74	50	4	192
07:55–08:00	75	73	47	6	201
08:00–08:05	53	90	59	5	207
08:05–08:10	52	97	52	4	205
08:10–08:15	51	95	49	5	200
08:15–08:20	63	73	26	0	162
08:20–08:25	70	78	39	2	189
08:25–08:30	76	49	43	4	172
08:30–08:35	71	64	53	2	190
08:35–08:40	63	79	44	3	189
08:40–08:45	59	66	58	0	183
08:45–08:50	43	66	57	2	168
Total	740	904	577	37	2258

Note: *Controlling approach, **Metered approach

The total volumes of the northern, southern, western and eastern approaches were 740, 904, 577 and 37 veh/h respectively, and the volumes on the eastern approach were extremely low.

Figure 4 shows the signal phase time changes in one-minute intervals and that the red signal occupied more than 60 seconds in the 120 seconds of cycle length between 07:15 and 08:20. Outside of that period, the green signal dominated.

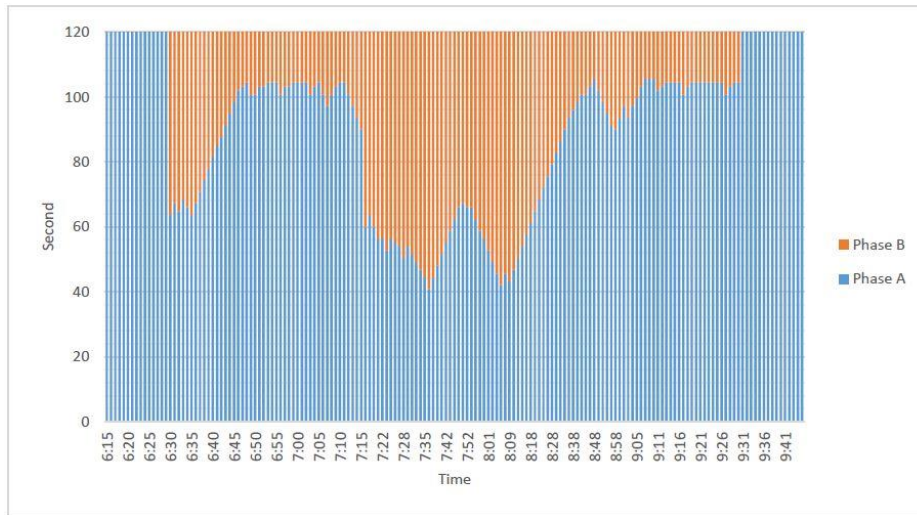


Figure 4. Signal phase time variations

However, queuing length on the southern approach is only longer than the detector location (115 meters) during the 08:15–08:45 periods, and metering was only operated during these periods.

4. METHODOLOGY

In order to find the optimum detector locations at TS351, the dataset collected using drones was used for queuing length measurement. For the AIMSUN modelling process, model construction, calibration and statistical tests are also required. Thus, four procedures were implemented, as depicted in Figure 5.

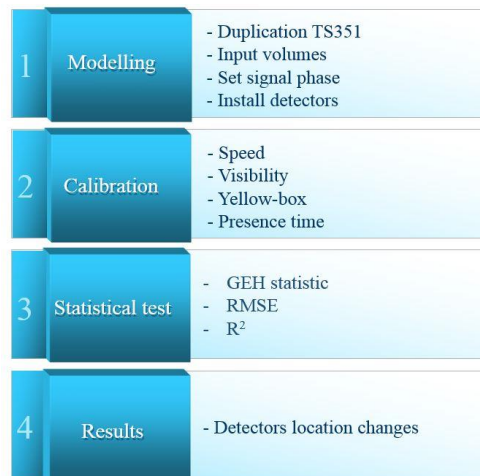


Figure 5. AIMSUN procedure

At the first stage, emulating TS351 was conducted, with input data such as traffic volume, signal phase time and location of detectors. Following the completion of the first stage, the maximum speed and visibility on each approach, yellow-box speed and detector presence time were calibrated to match queuing lengths on each approach. In the third stage, AIMSUN outputs were evaluated using GEH, RMSE and R^2 tests. The final stage simulates the optimum detector locations in relation to queuing length. In order to investigate a variety of traffic conditions, 10 replications were simulated in each peak period and their average queuing length further analyzed.

5. MODELLING

5.1 Modelling of TS351

In this research, the existing traffic circumstances, including network layout, traffic volumes, signal control schemes, driver behavior, and public transport (bus), were represented in AIMSUN 7. For the layout modelling, TS351 was extracted using the function “template create” in AIMSUN 7 and the scale was matched on Google Maps as depicted in Figure 6. After the modelling process, four centroids that generate and attract vehicles were connected to each approach. In AIMSUN, each centroid has an endemic number, for instance, 2029 (northern), 2030 (eastern), 2031 (southern) and 2032 (western). In addition, TS351 is composed of a 5% uphill gradient from the northern approach to the southern approach. Thus, this grade was applied using the function “altitude” (slope percentage).



Figure 6. TS351 in AIMSUN

Bus route 171 runs along the western and northern approaches in both directions in 30-minute service intervals during the morning peak periods. Thus, the bus stops (yellow square in Figure 6) using the “create a public transport stop” function was put on the western approach in both directions at 250 meters from TS351. Then, 30-minute service intervals for buses was selected using the connection with the public transport plan. In terms of the detector setting, ramp metering function was used to place the detector on the southern approach at a distance of 115 meters for the morning peak periods. Further, 4.5 meters of detector length (i.e. the

standard size in Adelaide) was applied (blue square in Figure 6). Two traffic signals were also installed near the stop line on the northern approach for the morning peak and western approach for the afternoon peak periods. In addition, stop lines were set back 10 meters for metering operation as the current stop-line position at TS351.

5.2 Input traffic volumes

Queuing lengths on each approach were calculated in five-minute intervals using the numerical model developed in this study. Traffic volume input with an example of the northern approach in the morning peak periods.

First, a one-hour origin-destination matrix for the northern approach was used as input, and then 8.6% of traffic volume on the basis of one-hour volumes was applied during the 07:50 to 07:55 five-minute period. The traffic volumes for the remaining periods and the afternoon peak were applied using the same method. In addition, 15 minutes of warm-up and cool-off periods were adopted before and after the one-hour modelling periods for more accurate queuing length simulation, queuing length dispersal and smooth vehicle movements.

5.3 Traffic management

The other essential aspect in AIMSUN modelling is the setting of control strategies for performance analysis. The installed detectors and traffic signals should be connected for metering roundabout operation in accordance with queuing length on the controlling approach. Thus, they were linked by traffic conditions under the “traffic management” function. The traffic condition was specified by two triggers (start and stop) that constantly monitored the queue detector zone occupancy time.

Traffic signals in the morning peak periods are operated by vehicle presence time on the detectors. According to TSS (2012), the value of occupancy for a detector is defined as the “percentage of cycle time that the detector detected presence in the last cycle” and it can be expressed as in Equation (1).

$$Occupancy = \frac{\sum_{i=1}^{Total\ number\ of\ intervals} t_{final}(i, cycle) - t_{init}(i, cycle)}{Cycle} \times 100 \quad (1)$$

Where $t_{init}(i, cycle)$ is an initial time,

$t_{final}(i, cycle)$ is a final time, and

Cycle is 120 seconds

In the morning peak, when the detector on the southern approach detects queuing lengths for three seconds, the traffic signal on the northern approach shows red sign. Thus, the occupancy value of 55 was input for detection start and a value of 20 was set for detection end. As detectors were installed on both lanes, when the queuing length hit one of detectors, the signal displays red.

A vehicle entering from the northern approach is blocked by a red signal (refer to Figure 7(a)) and Figure 7(b) shows normal vehicle movements when the queuing length does not reach the detector.



(a) Red sign on the northern approach



(b) Green sign on all approaches

Figure 7. Signal operation in the morning peak periods by queuing length

5.4 Control plan

The “trigger” function was used to connect the signal phase to the “traffic management” function, as described in the section above. In order to duplicate the real-life signal phase timing of TS351, two control plans for each peak period were applied. TS351 was set to a double-cycle operation in the morning peak periods with the cycle time totaling 120 seconds. Two control plans for the morning peak periods can be defined as below:

- Control Plan 1: Queuing length is shorter than detector location
- Control Plan 2: Queuing length is longer than detector location

Control Plan 1 was specified as a default plan, to be used when vehicle queues did not extend to the detector on the controlling approach (e.g. detector on the southern approach for morning peak). In this case, a minimum green time of 42 seconds (21 + 21 seconds) and maximum green time of 90 seconds (45 + 45 seconds) were coded in during the morning peak periods. This resulted in an average green time of 67 seconds in the morning peak, which matched the SCATS signal operation for the site.

Control Plan 2 was used during signal metering operation. This happens when the vehicle queuing length on the southern approach reaches the detector and it is occupied for longer than the prescribed occupancy time.

If this condition is met, AIMSUN would automatically switch to Control Plan 2 and go back to Control Plan 1 once the detector occupancy was cleared. Signal phase settings for Control Plan 2, which shows that minimum green times during the signal metering operation were reduced from 42 seconds to 28 seconds in order to provide more capacity for the controlling approach.

6. CALIBRATION

In terms of calibration in a microscopic simulation model, three types of parameters usually need to be adjusted: network parameters, vehicle parameters and driver parameters (Yin & Qiu 2011). Similar to other microscopic models, AIMSUN classifies global network parameters, local section parameters and vehicle parameters as its major parameters (Septarina 2012). The three parameters in AIMSUN can be represented as below (TSS 2012):

- Global parameters: These parameters affect all types of vehicles (e.g. reaction time, lane change, car following).

- Local section parameters: These parameters affect all types of vehicles passing through a specific section of the network (e.g. speed limit, visibility distance).
- Vehicle parameters: These parameters affect particular types of vehicles driven in the whole network (e.g. maximum desired speed, maximum acceleration).

In the calibration, the default values of the global parameters were not adjusted because TS351 is a small area, and no other parameters would affect its operation. Thus, unified global parameter values such as reaction time, lane change and car following were applied for the measurement of queuing lengths on each approach. To match the queuing length from the drone survey data, local section and vehicle parameters were calibrated as summarized in Table 3.

Table 3. Adjusted parameters in AIMSUN

Parameters		Default value	Adjusted value
Local section parameter	Maximum speed (approaching)	60 km/h	50 km/h (western)
	Maximum speed (exiting)	60 km/h	36 km/h (northern)
	Visibility distance	10 m	6 m (northern)
			12 m (southern)
8 m (western)			
Yellow-box speed	10 km/h	4 km/h (northern) 5 km/h (southern)	
Vehicle parameter	Maximum desired speed (bus)	100 km/h	60 km/h
	Maximum desired speed (vehicle)	120 km/h	60 km/h

6.1 Local section parameter

Local section parameters influence vehicles driving in a particular section. The calibrated local section parameters and their descriptions are presented below.

- Maximum speed (approaching approach)

The default value for maximum speed is 60 km/h on each approach. In the morning peak, driving distractions from the western approach occur due to sunrise. Thus, a decrease of 10 km/h (50 km/h) was input.

- Maximum speed (exiting approach)

In the morning, the majority of vehicles from the southern and western approaches head towards the northern exiting approach, furthermore, the northern approach consists of a short lane. Consequently, traffic congestion occurs at the northern exiting approach. Thus, 36 km/h of maximum speed was applied. In respect to the southern exiting approach, two lanes become one lane, thus, 40 km/h of maximum speed was specified.

- Visibility distance

Security of sight when vehicles are moving is important, especially when entering the roundabout, to check vehicle movements from the other approaches. In AIMSUN, visibility

distance plays the role of this function. In the morning, similar to the maximum speed (approaching), drivers from the western approach have trouble entering TS351 due to sun glare, thus eight meters of value was input. In addition, TS351 consists of five per cent of uphill from the northern to the southern approach. As a result, six and 12 meters of visibility distance were applied for the northern and southern approaches respectively.

- Yellow-box speed

Yellow-box speed is a unique function dealing with vehicle departure in the roundabout circulating section in AIMSUN. When vehicles enter the roundabout, they must avoid conflict with vehicles that have already entered the roundabout. Thus, approaching vehicles enter the roundabout when the preceding vehicle is below the yellow-box speed parameter. In morning peak periods, traffic volume on the southern approach was higher than the other approach and vehicles tended to enter the TS351 with a shorter acceptance time. Moreover, queuing length on the northern approach was longer than the other approaches. Thus, 5 km/h and 4 km/h of yellow-box speed were specified in the morning peak.

6.2 Vehicle parameter

Vehicle parameter influences a specific type of vehicle when driving in the network. In AIMSUN, default values of maximum desired speed for buses and passenger vehicles are set with 100 km/h and 120 km/h respectively. However, the speed limit of all approaches near TS351 is 60 km/h. Therefore, 60 km/h for buses and passenger vehicles was input for AIMSUN calibration.

6.3 Occupancy value adjustment

In Section 5.3, the metering system was set with 55 as the occupancy value on each lane. This value was slightly increased to 57, as that fitted the queuing length. Thus, when the occupancy value is above 57, the traffic signal on the northern approach changes to red.

6.4 Phase time adjustment

With respect to signal time setting, minimum and maximum green time were specified based on SCATS SM data in Section 5.4. In the morning peak periods, two seconds of minimum green time and four seconds of maximum green time were added in Control Plans 1 and 2.

7. RESULTS

Table 4 shows the AIMSUN results of queuing length on each approach after the calibration process and matching ratio versus the survey results. In regard to the matching ratio, the ranges of 63–89, 48–100, 76–94 and 68–97% were simulated on the northern, eastern, southern and western approaches respectively.

Table 4. Queuing length comparison: survey data and AIMSUN

Time	**Northern (m)			Eastern (m)			*Southern (m)			Western (m)		
	S	A	Ratio	S	A	Ratio	S	A	Ratio	S	A	Ratio
8:15–8:20	1003	908	89%	0	0	100%	153	162	94%	128	96	68%
8:20–8:25	835	724	85%	7	7	100%	170	182	94%	200	184	91%
8:25–8:30	507	586	86%	7	14	50%	128	144	89%	120	154	77%
8:30–8:35	650	552	82%	10	21	48%	155	158	99%	220	210	96%
8:35–8:40	60	88	68%	7	7	100%	180	158	86%	273	260	95%
8:40–8:45	45	72	63%	0	0	100%	140	112	76%	273	264	97%

Note: *Controlling approach and ** Metered approach

S = survey result; A = AIMSUN output

7.1 Statistical tests result

Table 5 summarizes the results of the statistical test between drone data and AIMSUN output. All GEH values are under five, meaning it is well calibrated.

Table 5. Results of statistic tests (drone survey data versus AIMSUN)

Statistic	Time	Northern	Eastern	Southern	Western
GEH	08:15–08:20	3.11	0.00	0.72	1.85
	08:20–08:25	3.98	0.00	0.90	1.05
	08:25–08:30	3.42	2.16	1.37	2.90
	08:30–08:35	4.00	2.79	0.24	2.15
	08:35–08:40	3.25	0.00	0.74	2.25
	08:40–08:45	3.53	0.00	1.57	2.16
Average GEH	08:15–08:45	3.54	0.82	0.92	2.06
RMSE	08:15–08:45	5.3m	1.73m	2.3m	4.6m
R ²	08:15–08:45	97.3%	80.3%	77.2%	93.1%

Moreover, RMSE and R² tests show TS351 in AIMSUN is also appropriately calibrated. For the northern approach, the RMSE value is the maximum (5.3 meters); however, R² describes that AIMSUN output fits the drone data with 97.3% accuracy. For the southern approach, R² matches the drone data with 77.2% accuracy. The GEH and RMSE values explain the southern approach, which is also well fit. Thus, it can be seen that AIMSUN outputs are reliable.

7.2 Optimal detector location

As mentioned earlier, a detector location of between 50 meters and 120 meters from the stop line is suggested for metering roundabout (Akçelik 2011). Thus, the detector was moved in AIMSUN from 50 meters to 225 meters in 25-meter increments. Then, average queuing length from 10 replications in five-minute increments for a total 30 minutes (08:15–08:45) is presented in Table 6.

Table 6. Queuing length according to detector location moves

Time	DL C = 50 m				DL C = 75 m			
	N (m)	E (m)	S (m)	W (m)	N (m)	E (m)	S (m)	W (m)
08:15–08:20	2744	0	47	186	1682	0	70	44
08:20–08:25	2550	7	32	302	1742	7	80	60
08:25–08:30	2008	7	40	288	1306	7	52	40
08:30–08:35	1862	7	42	318	1424	7	60	52
08:35–08:40	962	14	28	362	486	14	76	68
08:40–08:45	924	0	30	350	424	0	70	70
Total	11050	35	219	1806	7064	35	408	334
N+E+S+W	26,220 m				15,682 m			
Time	DL C = 100 m				DL C = 125 m			
	N (m)	E (m)	S (m)	W (m)	N (m)	E (m)	S (m)	W (m)
08:15–08:20	1256	0	125	82	862	0	166	102
08:20–08:25	922	7	144	124	700	7	188	180
08:25–08:30	782	7	122	124	568	14	150	164
08:30–08:35	752	7	128	162	554	21	168	220
08:35–08:40	180	14	134	170	82	7	176	268
08:40–08:45	142	0	100	174	76	0	124	260
Total	4034	35	753	836	2842	49	972	1194
N+E+S+W	11,316 m				10,114 m			
Time	DL C = 150 m				DL C = 175 m			
	N (m)	E (m)	S (m)	W (m)	N (m)	E (m)	S (m)	W (m)
08:15–08:20	824	0	188	116	554	0	202	134
08:20–08:25	656	14	194	190	660	21	216	200
08:25–08:30	522	25	160	164	530	28	184	188
08:30–08:35	526	28	162	226	550	28	180	242
08:35–08:40	80	28	170	282	80	21	198	306
08:40–08:45	80	0	130	282	76	0	151	296
Total	2688	95	1004	1260	2450	98	1131	1366
N+E+S+W	10,094 m				10,090 m			
Time	DL C = 200 m				DL C = 225 m			
	N (m)	E (m)	S (m)	W (m)	N (m)	E (m)	S (m)	W (m)
08:15–08:20	480	0	238	152	520	0	254	168
08:20–08:25	560	21	224	264	550	21	250	298
08:25–08:30	520	28	206	224	500	28	236	254
08:30–08:35	520	28	184	260	510	28	222	288
08:35–08:40	42	21	228	268	42	42	242	288
08:40–08:45	46	0	172	312	46	0	202	340
Total	2168	98	1252	1480	2168	119	1406	1636
N+E+S+W	9,996 m				10,658 m			

Note: N = northern; E = eastern; S = southern; W = western

The optimal detector location should reflect the minimum queuing length considering all approaches. Figure 8 illustrates the queuing length results in AIMSUN based on detector location changes.

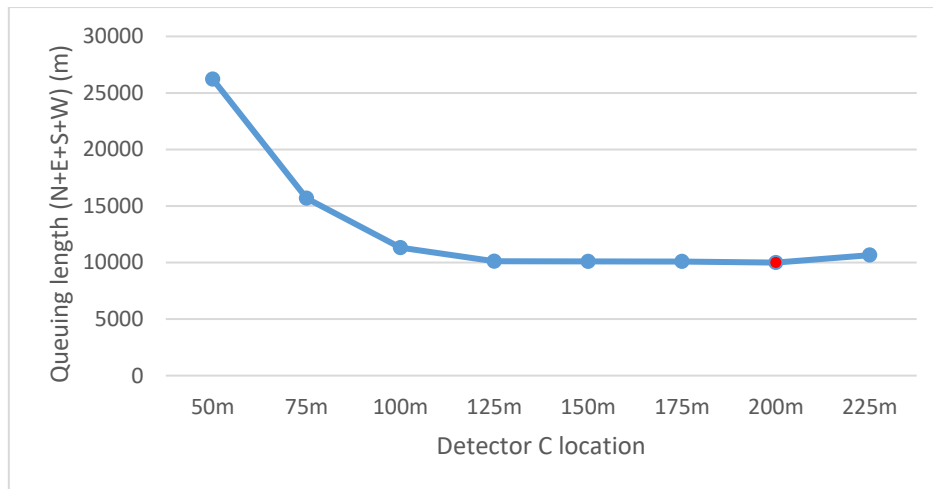


Figure 8. Queuing length according to detector location changes in AIMSUN

When the detector was at 50 meters, queuing length considering all approaches (northern + eastern + southern + western) was at the maximum of 13,110 meters for 30 minutes. When the detector was located between 50 and 100 meters from the stop line the queuing length reduced significantly. Detector location at 100 meters to 200 meters decreased the queuing length slightly, while detector at 220 meters resulted in a longer queuing length.

When the detector is at 200 meters, the total queuing length for 30 minutes is 4,998 meters. On the other hand, the current location of detector (115 meters) generated 5,217 meters of queuing length. Thus, 273 meters of queuing length can be reduced by relocating detector. However, when the detector is at 50 meters, 7,893 meters of queuing length can be generated.

8. CONCLUSION AND FUTURE WORK

As roundabouts can result in traffic congestion due to unique operation patterns, called unbalanced traffic conditions, metering roundabouts are receiving growing attention. However, few studies have focused on detector locations at metering roundabouts.

Therefore, this study attempted to find the optimal detector location to optimize queuing at an entire metering roundabout using microscopic simulation model AIMSUN. Moreover, modelling and calibration methods were reported based on TS351 with drone survey data for queuing length, SCATS data for traffic volumes and signal phase time, and DPTI documents for detector location and vehicle presence time on the detector.

The results based on AIMSUN model output demonstrate that the optimal detector location at TS351 is 200 meters, which is not within the range of 50–120 meters currently recommended. In addition, there are several other findings:

- Shorter detector location decreases the queuing length on the controlling (southern) approach and increases the queuing length on the metered (northern) approach.
- A 50-metre change in detector location increases the maximum queuing length considering all approaches.
- At 200 meters, detector location results in the minimum queuing length considering all approaches.

Although this paper studied only one case of a metering roundabout, it can be expected that when other metering roundabouts are considered this paper can be used to determine detector location using AIMSUN software. Future research on a variety of metering roundabouts, using different microscopic simulation models, is needed.

References

- Ahn, W-Y 2012, 'A Study on Roundabout Signal Metering Operation by Considering Entry Lane's Traffic Volume', *International Journal of Highway Engineering*, vol. 14, no. 2, pp. 175-181. (in Korean)
- Akçelik, R 2004, 'Roundabouts with unbalanced flow patterns', *ITE 2004 Annual Meeting*, Florida, USA.
- Akçelik, R 2005, 'Capacity and performance analysis of roundabout metering signals', *TRB National Roundabout Conference*, Vail, Colorado, USA, pp. 22-25.
- Akçelik, R 2006a, 'Analysis of Roundabout Metering Signals', *Paper presented at the 25th AITPM 2006 National Conference*, Melbourne, Australia.
- Akçelik, R 2006b, 'Operating cost, fuel consumption and pollutant emission savings at a roundabout with metering signals', *ARRB 22nd Conference*, Canberra, Australia.
- Akçelik, R 2011, 'Roundabout metering signals: capacity, performance and timing', *Procedia-Social and Behavioral Sciences*, vol. 16, pp. 686-696.
- Geers, DG, Tyler, P, Hengst, B, Huang, E & Quail, D 2009, 'Enhanced Roundabout Metering', *16th ITS World Congress and Exhibition on Intelligent Transport Systems and Services*, Stockholm, Sweden.
- Hummer, JE, Milazzo, I, Joseph, S, Schroeder, B & Salamadi, K 2014, 'The Potential for Metering to Help Roundabouts Manage Peak Period Demands in the US', *Transportation Research Board 93rd Annual Meeting*, Washington D.C, USA.
- Stevens, CR 2005, 'Signals and Meters at Roundabouts', *Paper presented at the 2005 Mid-Continent Transportation Research Symposium*, Iowa, USA.
- TSS 2012, *Aimsun 7 Dynamic Simulators User's Manual*, Version.
- Zadid, M & Yue, W 2009, 'Comparison of a roundabout model using AASIDRA and PARAMICS', *Australasian Transport Research Forum (ATRF), 32nd, 2009. The Growth Engine: Interconnecting Transport Performance, the Economy and the Environment*, Auckland, New Zealand.